

**Atomic structure of Si nanowires on Ag(110): A density-functional theory study**

Guo-min He

*Department of Physics, Xiamen University, Xiamen 361005, China*

(Received 15 April 2005; revised manuscript received 23 August 2005; published 11 January 2006)

We have systematically investigated the adsorption of Si on the Ag(110) surface employing density-functional theory. Various adsorption geometries have been considered for Si coverages up to 2.0 monolayers. Our results show that the Si-Ag bonds are slightly more favorable than the Si-Si bonds at low Si coverage and an attractive interaction between the Si adatoms is also identified. From the calculated results, we identify the most possible atomic structures of Si nanowires on the Ag(110) surface and propose a reasonable mechanism for the growth of Si nanowires on the Ag(110) surface.

DOI: [10.1103/PhysRevB.73.035311](https://doi.org/10.1103/PhysRevB.73.035311)

PACS number(s): 68.43.Bc, 68.65.La, 71.15.Mb

**I. INTRODUCTION**

Semiconductor nanostructures, such as nanowires and nanodots, are receiving more and more attention for their potential applications in mesoscopic research and electronic nanodevices. Among them Si nanowires (Si NWs) have attracted much attention due to their compatibility with the conventional Si-based technology. Up to now considerable effort has been devoted to synthesizing Si nanowires by employing various different methods including chemical vapor deposition (CVD) with metallic catalysts or oxide assistance,<sup>1-3</sup> laser ablation or simple evaporation,<sup>4-6</sup> or photolithography technology combined with etching.<sup>7</sup>

Recently, an experimental analysis using scanning tunneling microscopy (STM) and low-energy electronic diffraction (LEED) as well as high-resolution core-level spectroscopy (HRCLS) and advanced synchrotron radiation photoemission (PES) has been performed on the Si/Ag(110) surface.<sup>8</sup> It was found that massively parallel one-dimensional Si nanowires have been grown by the deposition of about 0.25 monolayers (MLs) of Si onto the Ag(110) surface. The experimental studies also demonstrated that there are some special features for the Si nanowires: (i) All Si NWs are perfectly aligned along the  $[\bar{1}10]$  direction of the Ag(110) surface and markedly asymmetric along their widths. Moreover, the Si NWs have the same definite width of 16 Å, and 5.77 Å periodicity along their lengths, which corresponds to a  $(2 \times 4)$  unit cell on the Ag(110) surface. (ii) All Si NWs have an identical and highly perfect atomic structure two atoms thick that comprise two and only two distinct silicon environments. (iii) The Si NWs show metallic character, revealing striking quantized states dispersing only along the length of the nanowires. It can be viewed as the direct evidence by experiment that doping is not needed for obtaining the conducting Si NWs.

In contrast, theoretical studies of Si on the Ag surface are rather limited. Virtually nothing is known about how Si is incorporated at the surface and assembled to nanowires, and what are the structures of the Si NWs. In order to better understand these issues we have studied the adsorption of Si on the Ag(110) surface employing density-functional theory. We report a systematic *ab initio* study of the coverage dependence of the physical and chemical properties of Si ad-

sorption on the Ag(110) surface. In the present work we focus mainly on the interaction of atomic Si with the Ag(110) surface for various Si adsorption geometries as a first step towards the understanding of the elementary processes of the formation of the Si NWs. The adsorption of Si on the Ag surface is also of fundamental interest in relation to understanding the nature of the Si-Ag bond in general.

This paper is organized as follows. The calculation details are given in Sec. II. Section III presents the calculated results for surface adsorption as a function of Si coverage. Finally, a brief summary is given in Sec. IV.

**II. CALCULATION DETAILS**

The density-functional theory total-energy calculations are performed with the SIESTA code (Ref. 9) within the local-density approximation (LDA). The Ceperley-Alder form of exchange and correlation energy function was used. The ion and core electrons were replaced by norm conserving pseudopotentials in their fully separable form, and numerical atomic orbitals are used as the basis sets. We first performed a series of calculations to optimize the basis sets for the Ag and Si atoms, as well as their respective pseudopotentials, until finally the bulk equilibrium properties of Ag and Si are compared reasonably well with the experimental values. For Ag and Si, we chose double zeta atomic orbitals plus polarization orbitals as the basis sets with an equivalent plane-wave cutoff of 180 Ry to represent the charge density.

The surface is modeled by a five-layer slab separated by a 14-Å vacuum space and Si is placed on one side of the slab. The positions of the top two Ag layers and Si adatoms are relaxed until the forces on the atoms are less than 0.02 eV/Å, while the bottom three layers of Ag atoms were held fixed in their bulk positions. In the  $(1 \times 1)$  surface unit cell, more than 20 special  $k$  points are used in the surface irreducible Brillouin-zone for the Brillouin-zone integration.

The stability of various  $\text{Si}_n/\text{Ag}$  structures is analyzed with respect to the adsorption energy. The adsorption energy is defined as

$$E_{ads} = E_{\text{Si}_n/\text{Ag}}^{slab} - E_{\text{Ag}}^{slab} - n_{\text{Si}}\mu_{\text{Si}}, \quad (1)$$

where  $E_{\text{Si}_n/\text{Ag}}^{slab}$  is the total energy of the  $\text{Si}_n/\text{Ag}(110)$  surface under consideration and  $E_{\text{Ag}}^{slab}$  is that of the reference

system—i.e., the clean Ag(110) surface.  $n_{Si}$  is the number of Si adatoms and  $\mu_{Si}$  is the chemical potential of Si. In the calculation of the adsorption energy  $\mu_{Si}$  is set equal to the bulk energy of Si in the diamond structure.

To help analyze the energetics of different structures, we compare the Si-Si binding  $E_{Si-Si}$  to the Si-Ag binding  $E_{Si-Ag}$ . For  $n$  Si adatoms adsorption on the Ag(110) surface (denoted as a  $Si_n$  cluster below), the  $E_{Si-Si}$  and  $E_{Si-Ag}$  are defined as

$$E_{Si-Si} = \frac{1}{n_{Si}} [E_{Si_n/Ag}^{slab} - n_{Si} E_{Si_1/Ag}^{slab} + (n_{Si} - 1) E_{Ag}^{slab}], \quad (2)$$

$$E_{Si-Ag} = \frac{1}{n_{Si}} [E_{Si_n/Ag}^{slab} - E_{Si_n} - E_{Ag}^{slab}], \quad (3)$$

where  $E_{Si_1/Ag}^{slab}$  is the total energy for the surface with a single Si adsorbed atom [Fig. 1(A1) was used to obtain the results of Fig. 4(b)]. The  $E_{Si_n}$  is the total energy of the  $Si_n$  cluster which is calculated from the same geometries of the adsorbed  $Si_n$  cluster on the Ag(110) surface—i.e., without optimizing. Thus the structure of a  $Si_n$  cluster is not the one corresponding to the global minimum of the  $Si_n$  cluster. According to the definition,  $E_{Si-Si}$  can be regarded as the energy required to dissociate the cluster into  $n$  noninteracting Si adatoms while  $E_{Si-Ag}$  is the energy required to separate the adsorbed system  $Si_n/Ag$  into two noninteracting parts: the clean Ag(110) surface and an independent  $Si_n$  cluster. It is also defined such that a positive value indicates that the interaction is repulsive and a negative value indicates that the interaction is attractive.

The calculated results of the ground-state properties for Ag and Si are listed in Table I. It can be seen that the results are comparable with the experimental values. Systemic underestimation of the lattice constants and overestimation of cohesive energy are typical for the LDA approximation. For the case of Si it agrees with these trends while for Ag it slightly underestimates the cohesive energy. Test calculations showed that the main reason for this is the use of limited basis sets in dealing with the Ag  $4d$  electrons. In addition, test calculations for some selected structures have been performed to check the convergence with respect to the  $k$ -point set, slab size, and vacuum thickness. The errors in adsorption energy due to the  $k$ -point set and vacuum thickness were estimated to less than 0.03 eV/atom. When the number of layers in the Ag slab is increased from 5 to 6, the adsorption energy changes as much as 0.05 eV/atom; however, the difference in adsorption energy between structures is within 0.03 eV/atom. Moreover, the bond length and geometric structure in comparison with the calculation of adsorption energy are not sensitive to the size of the simulation cell. Combining all these tests, we make an estimate of the numerical uncertainty of 0.05 eV for the adsorption energies. It should be noted that only some selected structures are tested. Since we study the relative stability of different structures by the difference between two adsorption energies, we believe the errors of absolute values would not affect the conclusion made in this work.

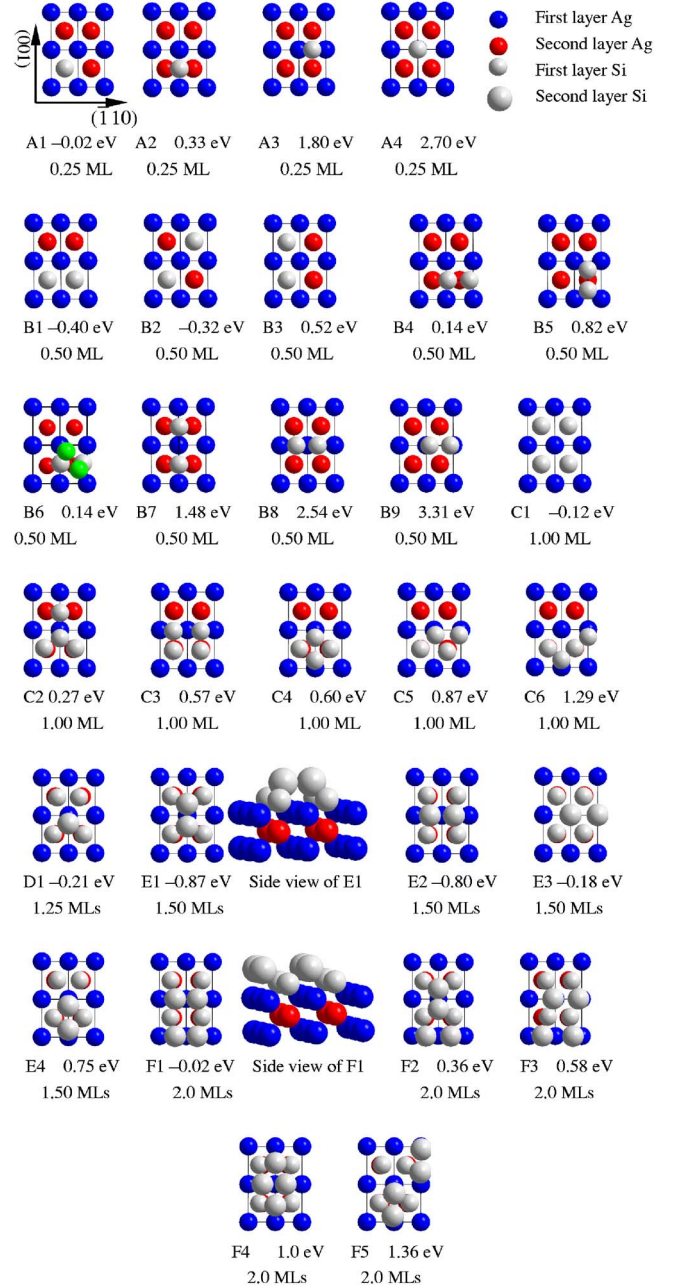


FIG. 1. (Color online) Possible atomic geometries of Si adsorption on the Ag(110) surface within the  $(2 \times 2)$  surface unit cell for various Si coverages (top view). Two (three for side view) surface layers of the Ag substrate including the Si adatoms are shown. The green balls of structure B6 indicate the initial position of the Si-Si dimer before relaxation while the grey balls indicate the final position after relaxation. The Si adatoms produced by the periodic-boundary conditions are omitted for clarity. The adsorption energies and Si coverages are also indicated.

### III. RESULTS AND DISCUSSIONS

Our investigations have been performed in two steps: in the first we explore in detail various possible structures for Si coverages ranging from 0.25 ML (one Si adatom) to 2.0 MLs (eight Si adatoms) using a  $(2 \times 2)$  unit cell, and identify the most favorable structures for a given Si coverage. In the

TABLE I. Bulk equilibrium properties of Si and Ag, including lattice constants  $a_0$ , bulk modulus  $B_0$ , and cohesive energy  $E_{coh}$ .

		$a_0$ (Å)	$B_0$ (Mbr)	$E_{coh}$ (eV)
Si	This work	5.40	0.95	5.75
	Expt. <sup>a</sup>	5.43	0.99	4.63
Ag	This work	4.10	92	2.85
	Expt. <sup>a</sup>	4.09	101	2.95

<sup>a</sup>Reference 10.

second step we consider many different atomic arrangements using a larger unit cell—i.e., a  $(2 \times 5)$  unit cell, and identify the structures of Si NWs.

### A. Coverage dependence of Si adsorption on the Ag(110) surface

The calculated results for coverage dependence of Si adsorption on the Ag(110) surface are summarized in Fig. 2 and also listed in Fig. 1. To model the structures of Si NWs, a sound knowledge of the Si adsorption behavior on the Ag(110) surface is essential. As a starting point, the adsorption of a single Si adatom on the Ag(110) surface has been calculated. We consider four adsorption sites: the hollow [Fig. 1(A1)], long bridge [LB, Fig. 1(A2)], short bridge [SB, Fig. 1(A3)], and top [Fig. 1(A4)] sites. The calculated adsorption energies  $E_{ads}$  are summarized in Table II and the corresponding structures are shown in Fig. 1. It can be seen that the hollow site [Fig. 1(A1)] is the energetically most favorable site with a adsorption energy of  $-0.02$  eV with respect to the bulk energy of Si. It should be noted that systemic overestimation of adsorption energy is the general trend of LDA results. This implies that the Si-Ag bond, if it is not more favorable over the Si-Si bond, is comparable with the Si-Si bond. Compared to the hollow site, both the long bridge [Fig. 1(A2)] and short bridge [Fig. 1(A3)] sites turn out to be less favorable. The vertical distance between Si and the first Ag surface layer ( $d_z$ ) is  $1.01$  Å for Fig. 1(A1) and the structure of Fig. 1(A4) is highly unfavorable, confirming that a maximum height of about  $2$  Å by experiment for the Si NWs corresponds to two atomic thicknesses. From Figs. 1(A1), (A2), and (A3) we estimate that the energy barrier for Si diffusion along the  $[\bar{1}10]$  surface direction—i.e., the well-known channel of the fcc(110) surface—is  $0.35$  eV

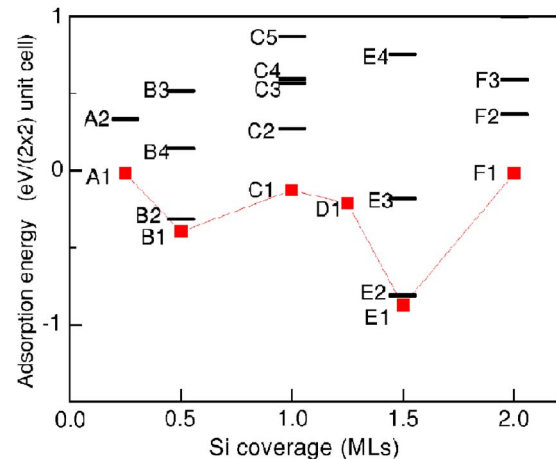


FIG. 2. (Color online) Calculated adsorption energies of Si on the Ag(110) surface per  $(2 \times 2)$  unit cell for various Si coverages with respect to the bulk energy of Si in diamond structure. The lowest adsorption energies are represented by squares in the figure. The solid lines connecting the calculated adsorption energies are used to guide the eyes.

while it is  $1.82$  eV for the diffusion across the channel in the  $[001]$  direction, indicating an anisotropic diffusion mechanism of Si on the Ag(110) surface.

To date no theoretical study for Si/Ag has appeared. However, other similar systems—e.g., Ge/Ag(110) (Refs. 11 and 12) or Si/Cu(110) (Ref. 13)—have been studied. It was found that Si has a negative adsorption energy of  $0.74$  eV on the hollow site of the Cu(110) surface, indicating that Si is more reactive on the Cu(110) surface than on the Ag(110) surface. This is consistent with the experimental results because the formation of a different type of surface alloys  $c(2 \times 2)$ -Si/Cu(110) had been reported.<sup>14,15</sup> For the case of Ge on the Ag(110) surface, the adsorption energy is calculated to be  $-0.35$  eV with respect to the bulk energy of Ge in diamond structure,<sup>11,12</sup> indicating that the Ge-Ag bonds are more favorable than the Ge-Ge bonds. This is not fully consistent with the experimental results because Ge nanoclusters were formed with the deposition of Ge on the Ag(110) surface, indicating that the Ge-Ge bonds are favorable instead.<sup>16</sup>

Turning now to higher coverage ( $\Theta=0.5$  ML), where there are two Si atoms per unit cell, we find that Fig. 1(B1) is the energetically most favorable structure. We also test the structures of the Si-Si dimer on the Ag(110) surface. Initially, the center of the Si-Si dimer with bond length of  $2.30$  Å is

TABLE II. The calculated adsorption energies and surface geometries of 0.25-ML Si at different surface sites on the Ag(110) surface. The energy differences ( $\Delta E_{ads}$ ) with respect to Fig. 1(A1) are also given. Here,  $d_z$  is the vertical distance between the Si adatom and the first Ag surface layer, and  $d_{Ag-Si}$  is the Ag-Si bond distance.

	Adsorption site	$E_{ads}$ (eV)	$\Delta E_{ads}$ (eV)	$d_z$ (Å)	$d_{Ag-Si}$ (Å)
Ag(110)	Hollow [Fig. 1(A1)]	$-0.02$	0.0	1.01	2.63
	Long bridge [Fig. 1(A2)]	0.33	0.35	0.92	2.42
	Short bridge [Fig. 1(A3)]	1.80	1.82	1.78	2.37
	Top [Fig. 1(A4)]	2.70	2.72	2.24	2.24

placed 3.0 Å above the hollow site [Figs. 1(B4)–(B6)], top site [Figs. 1(B7) and (B8)], short bridge site [Fig. 1(B9)], and long bridge site (not shown). Then structure optimizations were performed for a variety of initial orientations for the Si-Si dimer. After relaxation, the structure of Fig. 1(B6) relaxed to Fig. 1(B4) while the structure above the long bridge site relaxed to Fig. 1(B1). Figures 1(B4)–(B9) are all higher in energy than Fig. 1(B1), indicating that the structure of Si-Si dimer is not the most favorable structure on the clean Ag(110) surface. As the Si coverage increases from 0.25 to 0.50 ML, the  $E_{ads}$  for the most stable structures increase, compared  $-0.40$  eV for Fig. 1(B1) to  $-0.02$  eV for Fig. 1(A1), suggesting that the interaction of Si with Si on the Ag surface is attractive (this will be shown in more detail in Fig. 4 below). So at higher Si coverage, the formation of Si dimer structure would become possible.

For the full coverage adsorption ( $\Theta=1$  ML), Fig. 1(C1) is found to be the most favorable with a adsorption energy of  $-0.12$  eV. In this structure Si adatoms occupy all the available hollow sites within the  $(2 \times 2)$  unit cell. We also test the possibility of forming  $Si_4$  clusters (similar to what we have done for the Si dimer at Si coverage of 0.25 ML). However, they are all higher in energy than Fig. 1(C1). Based on the points that (i) the Ag-Si bonds are slightly more favorable than the Si-Si bonds; (ii) the structures of the  $Si_4$  clusters are not favorable, and (iii) the structure of Fig. 1(C1) is still exothermic, we conclude that the structure of Fig. 1(C1) is able to form at the low Si coverage regime and the first atomic layer in the Si nanowires—i.e., the interface between Si and the Ag substrate—would be eight Si adatoms occupying all the available hollow sites inside the  $(2 \times 4)$  unit cell on the Ag(110) surface, which represents a continuation of the bulk stacking sequence. Therefore for Si coverage higher than 1 ML, we calculate the adsorption energy for structures with additional one ( $\Theta=1.25$  MLs), two ( $\Theta=1.5$  MLs), and four ( $\Theta=2.0$  MLs) Si adatoms on the structure of Fig. 1(C1).

We now consider one additional Si adatom adsorption on the structure of Fig. 1(C1) (i.e.,  $\Theta=1.25$  MLs). Initially a variety of possible adsorption sites were tested. It was found that Si adsorption directly above the first layer Si is unstable and tends to relax to the furrow formed by the first layer Si. Therefore we calculate the energy profiles for Si migration along the furrow formed by the first layer Si in the  $[\bar{1}10]$  and  $[001]$  direction—i.e., from the SB site to the top site, and from the top site to the LB site. The diffusion paths are indicated by the arrows in the inset of Fig. 3. In the calculation the second layer Si adatom was placed in a position along the diffusion path and only allowed to relax in direction normal to the Ag(110) surface. The results are shown in Fig. 3. They were calculated as the total-energy difference between a Si adatom placed in a given site along the diffusion path and in the most stable adsorption site [Fig. 1(D1)]. From the calculated energy profile we find that the most favorable site is in a position between the top and LB site [Fig. 1(D1)] (denoted as LB2). The activation barrier is less than 0.1 eV from the SB site to the top site and about 0.25 eV from the top site to the LB site, suggesting that it is very mobile for the second layer Si adatoms. Moreover, at typical growth temperatures a second layer Si adatom may diffuse

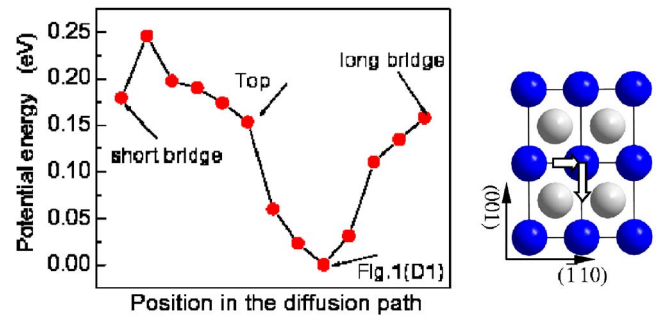


FIG. 3. (Color online) The total energy difference for a single Si adatom on the structure of Fig. 1(C1) at different positions along the diffusion path in the  $[\bar{1}10]$  and  $[001]$  direction. The diffusion path is also indicated by the arrows in the inset.

easily along the  $[\bar{1}10]$  direction and spontaneous trap in the LB2 site.

For the case of additional two and four Si adatoms adsorption on the structure of Fig. 1(C1) (i.e.,  $\Theta=1.5$  and 2.0 MLs, respectively), we have considered all possible site combinations of the hollow, SB, LB, LB2, and top sites. We also tested the possibility of the Si dimer structure (similar to what we have done for the Si dimer at Si coverage of 0.25 ML). It was found after extensive test that Figs. 1(E1) and 1(F1) are the most stable geometries at Si coverage of 1.5 and 2.0 MLs, respectively. From Fig. 2 it can be seen that Fig. 1(E1) is also the most favorable structure of all the geometries considered.

In order to aid our discussion concerning the bonding mechanism for Si adsorption on the Ag(110) surface, we compare the adsorbate-adsorbate interaction  $E_{Si-Si}$  to adsorbate-surface interaction  $E_{Si-Ag}$ , according to Eqs. (2) and (3). It is worth noting that the basis-set superposition error (BSSE),<sup>17,18</sup> which is inherent to the atomic orbital based self-consistent calculations, can introduce an error into the  $E_{Si-Ag}$ . We have used counterpoise corrections to estimate this error.<sup>17</sup> The total energy for  $E_{Si_n/Ag}^{slab}$  was first calculated; then the energies for the separated substrate  $E_{Ag}^{slab}$  and the adsorbate  $E_{Si_n}$  were calculated by ghosting the appropriate set of atoms. In this way the total system ( $E_{Si_n/Ag}^{slab}$ ) and its separated constituents ( $E_{Ag}^{slab}$  and  $E_{Si_n}$ ) have exactly the same basis set in the calculation.<sup>19</sup> Our results of  $E_{Si-Si}$  and  $E_{Si-Ag}$  for selected structures are summarized in Fig. 4. From Fig. 4(a) it can be seen that the Si-Ag interaction is attractive. The BSSE corrections behave as expected reducing the interaction energy compared with that of no BSSE corrections. Including the BSSE corrections, the variation of  $E_{Si-Ag}$  as a function of the Si coverage is rather similar to that without BSSE corrections. As the Si coverage increases, the attractive Si-Ag interaction decreases significantly. The decrease of  $E_{Si-Ag}$  at low Si coverage is due primarily to the energy gain of the Si-Si interaction within the  $Si_n$  clusters (i.e.,  $E_{Si_n}$ ). From a single Si adatom in Fig. 1(A1) to the Si dimer in Fig. 1(B1), the energy gain of  $E_{Si_n}$  is by as much as 3.50 eV/atom. At high Si coverage as more Si adatoms adsorb on the Ag(110) surface, more Si adatoms will share bonding with the same surface Ag atoms. Thus the so-called

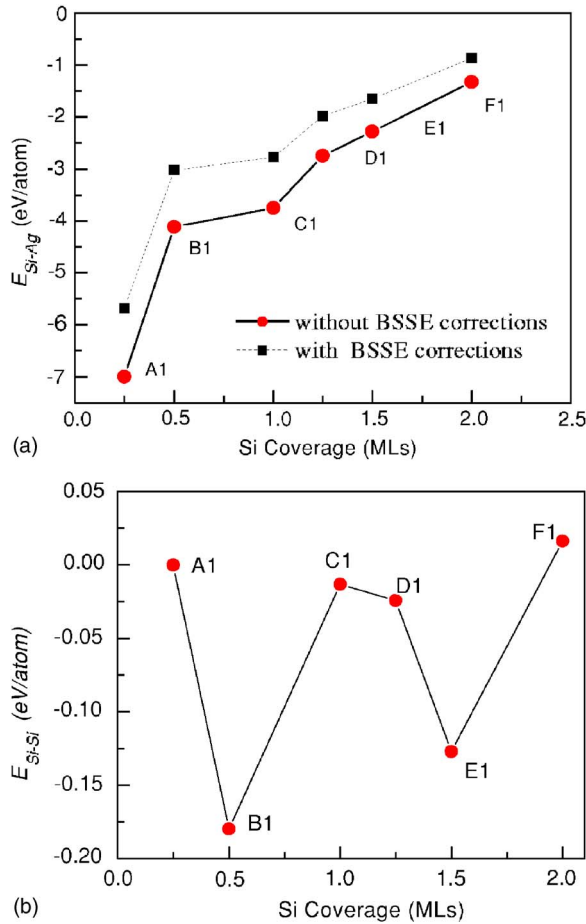


FIG. 4. (Color online) The calculated results for  $E_{Si-Si}$  and  $E_{Si-Ag}$  (in eV/atom) for selected structures in Fig. 1. The results with basis-set superposition error (BSSE) corrections for  $E_{Si-Ag}$  are also listed.

bonding competition effect will cause additional decrease of  $E_{Si-Ag}$ . Note that the clean Ag(110) surface and the  $Si_n$  clusters are not optimized in the calculation, and it will result in a slight overestimation of the interaction energy  $E_{Si-Ag}$ . Turning now to the adsorbate-adsorbate interaction  $E_{Si-Si}$ , we find that the Si-Si interaction is also attractive [cf. Fig. 4(b)]. The exception is for Fig. 1(F1) at Si coverage of 2.0 MLs where the Si-Si interaction becomes slightly repulsive. It is worth noting that Figs. 1(B1) and (E1), which are the respective most favorable structures at Si coverage of 0.5 and 1.50 MLs, have larger Si-Si interaction than those at other coverages. We also analyzed the bonding properties of  $Si_n/Ag(110)$  by the charge-density difference for some selected structures in Fig. 1 (not shown), which was obtained by subtracting the charge densities of the  $Si_n$  and the clean Ag(110) surface from that of  $Si_n/Ag(110)$ . It was found that electrons accumulate in the region between Si and the nearest Ag as well as between Si and Si. This suggests the formation of covalent bonds for both Si-Si and Si-Ag bonds.

On the basis of the above calculated results, we obtain the following understanding regarding the adsorption behavior of Si on the Ag(110) surface: (i) The formation of structure Fig. 1(C1) is possible because the Si-Ag bonds are slightly more favorable than Si-Si bonds at low Si coverage. (ii) The

barrier for Si diffusion on the clean Ag(110) is about 0.35 and 0.25 eV on Fig. 1(C1), indicating the high mobility of Si adatoms on the Ag(110) surface. (iii) The interaction of Si with Si is attractive, therefore a Si dimer structure would become favorable at high Si coverage as the Si-Ag bond becomes weak due to the bonding competition effect. (iv) The high stability of Figs. 1(B1) and (E1) can serve as building blocks of Si NWs observed in the experiment.

### B. Atomic structures of the SiNWs

To obtain the real atomic structures of the Si NWs, we now use a larger surface unit cell in the calculation—i.e., a  $(2 \times 5)$  unit cell. We focus on structure stability of the  $Si_n$  clusters for  $n$  varying from 12 to 18, which correspond to the Si coverages ranging from 1.2 to 1.8 MLs. Again, structure optimizations were performed for a variety of initial configurations. The results are listed in Fig. 5 and shown in Fig. 6. We find that Fig. 5(g1) turns out to be the most stable structure with Fig. 5(g2) almost degenerate in energy [the structure of Fig. 5(g2) is only 0.04 eV higher in energy than Fig. 5(g1)]. For Si coverages ranging from 1.2 to 1.8 MLs the adsorption energies decrease markedly, indicating that it is less favorable for more Si adatoms to adsorb on the structure of Fig. 5(g1). It is worth noting that for the formation of the first Si layer the adsorption energies first increase [Figs. 5(a1)–(c1)] and then decrease [Figs. 5(d1)–(f1)] when the Si adatoms consecutively occupy all the hollow sites inside the  $(2 \times 5)$  unit cell, indicating that (i) the growth of Si NWs along the  $[001]$  direction is less favorable; and (ii) the formation of Fig. 5(c1) is favorable in energy, which can be regarded as an important step to Fig. 5(g1). The detail geometries of Figs. 5(g1) and (g2) are listed in Table III. The structure of Fig. 5(g1) is consistent with the results of experimental observation that the Si NWs are markedly asymmetric along their widths with only two distinct silicon environments. It should be emphasized here that the structures in Fig. 5 with Si coverages less than 1.0 ML [e.g., Figs. 5(c1)–(f1)] do not correspond to the respectively most stable structures. For example, a two-Si-layer structure similar to Fig. 1(E1) is more favorable than Fig. 5(f1) at Si coverage of 1.0 ML; and a two-separated-rows structure like Fig. 1(B1) is more favorable than Fig. 5(c1) at Si coverage of 0.4 ML.

In order to gain deeper insight to the bonding properties of the Si NWs, we analyzed the local density of states (LDOS) for the structure of Fig. 5(g1), which is the most possible candidate for the Si NWs. The calculated results are shown in Fig. 7. The Fermi level is chosen as zero of energy. In Fig. 7 we only show the results for the energy range from  $-4.0$  to  $1.0$  eV where the experimental results exist. After analyzing the LDOS we found that the Si- $3s$  states hybridized with Si- $3p$  and Ag- $4d$  states give the contribution mainly in the range of  $-7.0$ – $-12.0$  eV. The LDOS of Ag before the adsorption of Si are dominated by the  $4d$  band centered at about 4.0 eV below the Fermi level, and they shift down to lower energy upon the adsorption of Si, indicating the existence of strong Si-Ag bonds. The electronic states below the Fermi level are mainly dominated by the Si  $3p$  states. Several electronic states centered around  $-0.80$ ,

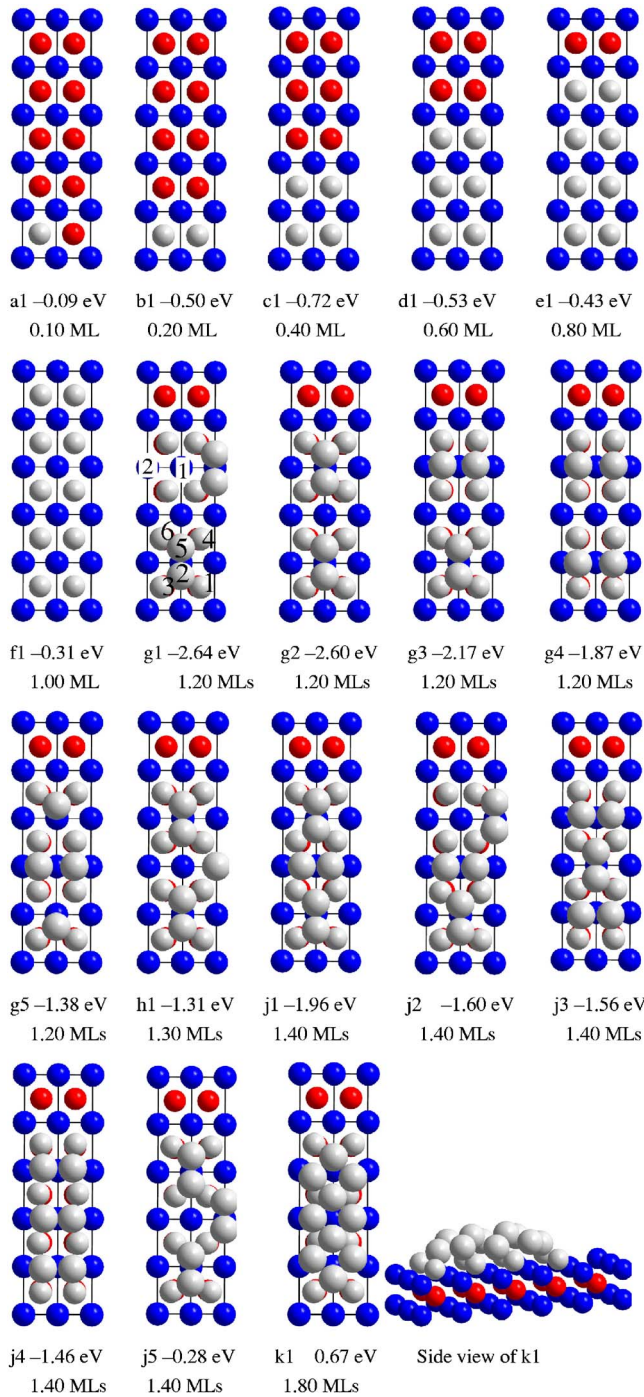


FIG. 5. (Color online) Possible atomic geometries of Si adsorption on the Ag(110) surface within the  $(2 \times 5)$  surface unit cell for various Si coverages (top view). Two (three for side view) surface layers of the Ag substrate including the Si adatoms are shown. The Si adatoms produced by the periodic-boundary conditions are omitted for clarity. The adsorption energies and Si coverages are also indicated. Note that c1, d1, e1, and f1 do not correspond to the respective most favorable structures for Si coverages below 1.0 ML.

$-1.26, -2.02, -2.60,$  and  $-3.03$  eV for the Si1 species, and  $-1.08, -2.0, -2.60,$  and  $-3.03$  eV for the Si2 species can be identified in Fig. 7. The valence-band spectra for the Si NWs

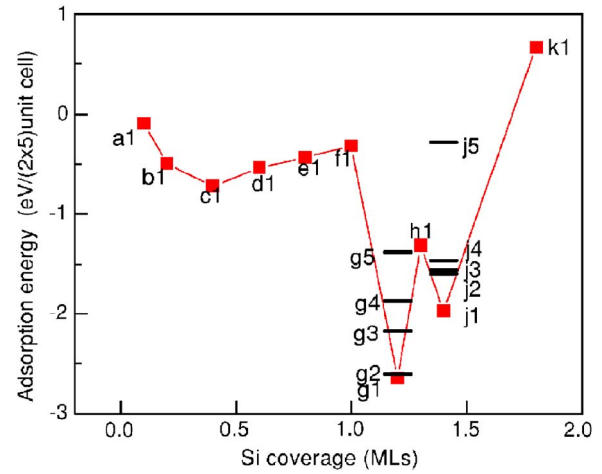


FIG. 6. (Color online) The calculated adsorption energies of Si on the Ag(110) surface for various Si coverages with respect to the bulk energy of Si. The solid lines connecting the calculated adsorption energies are used to guide the eyes. Note that c1, d1, e1, and f1 do not correspond to the respective most favorable structures for Si coverages below 1.0 ML.

have been recorded experimentally.<sup>8</sup> Compared to the clean Ag(110) surface, it was found that four new states appear in the valence band of the Si NWs—i.e., 0.92, 1.45, 2.37, and 3.12 eV below the Fermi level. From Fig. 7 we can find that (i) the new electronic states are mainly contributed by the Si 3p states; (ii) the electronic states centered around  $-0.80$  and  $-3.03$  eV for the Si1 species, and  $-1.08$  and  $-3.03$  eV for the Si2 species are quite close to the experiment values—i.e.,  $-0.92$  and  $-3.12$  eV. The difference is slightly larger between the calculated and experimental results for other electronic states centered around  $-2.0$  eV; (iii) the Si NWs are metallic with important contributions from the Si 3p states around the Fermi level. From surface band structure of Fig. 5(g1) (not shown) it is also confirmed that quantized states disperse only along the length of the nanowires, which is consistent with the experiment. On the basis of the points that (i) the atomic and electronic structures are overall in agreement with the experimental results, and (ii) of all the

TABLE III. The main geometrical parameters of g1 and g2 in Fig. 5. Units are in Å for bond lengths and degree for bond angles.  $d_z$  is the vertical distance. The atomic indexes for g2 are similar to g1.

Structure	Fig. 5(g1)	Fig. 5(g2)
$d_z$ (Si1-Ag)	1.145	1.146
$d_z$ (Si2-Ag)	2.500	2.480
$d_z$ (Si1-Si2)	1.355	1.354
Si1-Si2	2.348	2.345
Si2-Si5	2.439	2.445
Si1-Ag	2.628	2.627
Si2-Ag	2.760	2.760
$\angle$ Si1-Si2-Si3	92.57	92.66
$\angle$ Si1-Si2-Si5	115.80	116.06

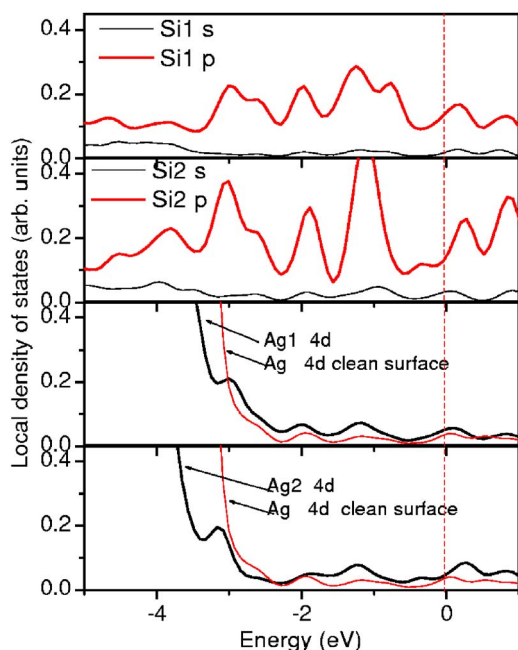


FIG. 7. (Color online) The local density of states (LDOS) for the Si and Ag atoms for Fig. 5(g1). The atomic indexes are indicated in Fig. 5(g1), and the thin lines in the last two panels are for the Ag atom of the clean surface. The Fermi level is set to the energy zero.

structures studied Fig. 5(g1) is the most favorable structure in energy, we conclude that the possible atomic structure of the Si NWs growth in the experiment is Fig. 5(g1).

From these data regarding the adsorption properties of Si on the Ag(110) surface we can derive the following picture of the self-assembled Si NWs on the Ag(110) surface (cf. Fig. 8). For a single Si adatom deposited on the Ag(110) surface it will first adsorb on a hollow site (A1). Then it diffuses along the  $[\bar{1}10]$  channel and joins another Si adatom to form the dimerlike structure (B1). Since the activation barrier is relatively small (about 0.35 eV) a Si adatom is mobile on the Ag(110) surface. It also has the possibility that they have formed the Si dimer structure before reaching the Ag(110) surface and finally relax to (B1) after the adsorption on the Ag(110) surface because the Ag-Si bonds favor slightly over the Si-Si bonds at low Si coverage. As more Si adatoms diffuse to meet them, these dimerlike structures then serve as the centers for the growth of the larger unit (C1). Next, newly incoming adatoms will climb up the monatomic-layer-high steps of C1 and finally form the most stable structure (E1). During the formation of E1, Si adatoms must ascend at the step edges of C1. It is an important atomic process that has been established by both experiment and theory<sup>20,21</sup> and regarded as an essential step up to nanoclusters.<sup>22</sup> We estimate the upward diffusion barriers to be about 0.4 eV using a  $(4 \times 3)$  surface unit cell, which is of the order of the diffusion barrier on the clean Ag(110) surface. Therefore it is feasible for the nucleation and growth of E1 under the typical growth conditions. Finally, the atomistic

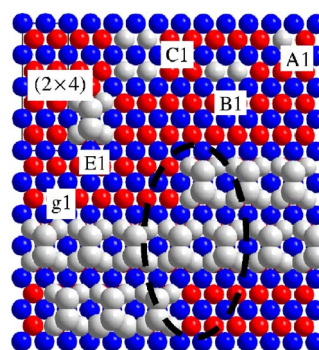


FIG. 8. (Color online) The important steps for the nucleation and growth of Si nanowires on the Ag(110) surface. The  $(2 \times 4)$  surface unit cell is also indicated. The circle indicates a feature visible in the experimental STM images in Ref. 8.

processes (A1-B1-C1-E1) repeat at adjacent site along the [001] direction, and E1 serves as a building block for the self-assembled Si NWs [Fig. 5(g1)]. According to the above atomistic processes, it is possible that the atomistic processes (A1-B1-C1-E1) repeat at an opposite adjacent site (indicated by the circle in Fig. 8(g1)), which is indeed visible in the experimental STM images<sup>8</sup> The Ag(110) surface has at least two effects for the growth of the Si NWs: (i) bind the Si adatoms strong enough to form the building block (E1), and (ii) provide an ideal anisotropy substrate for aligning the nanowires. Since the structure of Fig. 8(g1) is very similar to that of a Si(100)- $(2 \times 1)$  surface, we now proceed to study the possibility of functionalization of these Si NWs with organic molecules.

#### IV. SUMMARY

The adsorption of Si on the Ag(110) surface, which is relevant to the initial stage of the formation of the SiNWs, has been investigated by *ab initio* total-energy calculations. Our results show that the Si-Ag bonds are slightly more favorable than the Si-Si bonds at low Si coverage, and a Si-dimer structure is not the most favorable structure on the bare Ag(110) surface. At high Si coverage, the Si dimer structure with proper arrangement becomes more favorable in energy due to the weakening of the Si-Ag bonds and an attractive interaction between the Si adatoms. From our results the most possible atomic structures of the Si nanowires on the Ag(110) surface are identified, and a reasonable mechanism for the growth of the Si nanowires on the Ag(110) surface is proposed. Our calculated results are in reasonable agreement with the available experimental results.

#### ACKNOWLEDGMENTS

The author gratefully thanks Shu-ping Li for offering the computational facilities. The Siesta Research Group is gratefully acknowledged for providing us the SIESTA code (<http://www.uam.es/departamentos/ciencias/fismateriac/siesta/>).

- <sup>1</sup>J. Kikkawa, Y. Ohno, and S. Takeda, *Appl. Phys. Lett.* **86**, 123109 (2005).
- <sup>2</sup>T. I. Kamins, X. Li, and R. Stanley Williams, *Appl. Phys. Lett.* **82**, 263 (2003).
- <sup>3</sup>N. Wang, Y. H. Tang, Y. F. Zhang, C. S. Lee, I. Bello, and S. T. Lee, *Chem. Phys. Lett.* **299**, 237 (1999).
- <sup>4</sup>Y. H. Tang, Y. F. Zhang, N. Wang, W. S. Shi, C. S. Lee, I. Bello, and S. T. Lee, *J. Vac. Sci. Technol. B* **19**, 317 (2001).
- <sup>5</sup>Y. F. Zhang, Y. H. Tang, N. Wang, D. P. Yu, C. S. Lee, I. Bello, and S. T. Lee, *Appl. Phys. Lett.* **72**, 1835 (1998).
- <sup>6</sup>Y. H. Tang, Y. F. Zhang, N. Wang, C. S. Lee, X. D. Han, I. Bello, and S. T. Lee, *J. Appl. Phys.* **85**, 7981 (1999).
- <sup>7</sup>H. I. Liu, D. K. Biegelsen, N. M. Johnson, F. A. Ponce, and R. F. W. Pease, *J. Vac. Sci. Technol. B* **11**, 2532 (1993).
- <sup>8</sup>C. Leandri, C. Le Lay, B. Aufray, C. Girardeaux, J. Avila, M. E. Davila, M. C. Asensio, C. Ottaviani, and A. Cricenti, *Surf. Sci.* **574**, L9 (2005).
- <sup>9</sup>D. Sanchez-Portal, P. Ordejon, E. Artacho, and J. M. Soler, *Int. J. Quantum Chem.* **65**, 453 (1999).
- <sup>10</sup>C. Kittel, *Introduction to Solid State Physics* (John Wiley & Sons, New York, 1986).
- <sup>11</sup>S. Sawaya, J. Goniakowski, and G. Tréglia, *Phys. Rev. B* **59**, 15337 (1999).
- <sup>12</sup>S. Sawaya, J. Goniakowski, and G. Tréglia, *Phys. Rev. B* **61**, 8469 (2000).
- <sup>13</sup>Guo-min He, Shu-ping Li, and Zicong Zhou, *Surf. Sci.* **553**, 126 (2004).
- <sup>14</sup>C. Polop, C. Rojas, J. A. Martín-Gago, R. Fasel, J. Hayoz, D. Naumovic, and P. Aebi, *Phys. Rev. B* **63**, 115414 (2001).
- <sup>15</sup>J. A. Martín-Gago, C. Rojas, C. Polop, J. L. Sacedón, E. Román, A. Goldoni, and G. Paolucci, *Phys. Rev. B* **59**, 3070 (1999).
- <sup>16</sup>C. Leandri, H. Oughaddou, J. M. Gay, B. Aufray, G. Le Lay, J. P. Biberian, A. Ranguis, O. Bunk, and R. L. Johnson, *Surf. Sci.* **573**, L369 (2004).
- <sup>17</sup>P. Valiron, and I. Mayer, *Chem. Phys. Lett.* **275**, 46 (1997).
- <sup>18</sup>S. B. Boys and F. Bernardi, *Mol. Phys.* **19**, 533 (1970).
- <sup>19</sup>Note that it is difficult to perform the BSSE corrections with the counterpoise correction method for structures with different Si coverages. So such parts of corrections are not included and it leads to some errors for the results of the Si-Ag interaction [Fig. 4(a)]. For the same reason the BSSE corrections had not been made for the results obtained by Eq. (1). Therefore caution has to be made when comparing the results with different Si coverages though the relative stability of structures with the same Si coverage would be affected to a lesser extent by the basis-set superposition error.
- <sup>20</sup>F. Buatier de Mongeot, W. Zhu, A. Molle, R. Buzio, C. Boragno, U. Valbusa, E. G. Wang, and Z. Zhang, *Phys. Rev. Lett.* **91**, 016102 (2003).
- <sup>21</sup>W. Zhu, Francesco Buatier de Mongeot, U. Valbusa, E. G. Wang, and Z. Zhang, *Phys. Rev. Lett.* **92**, 106102 (2004).
- <sup>22</sup>K. Fichthorn and M. Scheffler, *Nature (London)* **429**, 617 (2004).